

VTI Anisotropy in the Jamieson and Echuca Shoals Formations in the Browse Basin

Aymen Beji

CSIRO
26 Dick Perry Ave
Kensington
WA 6151
Australia
aymen.beji@csiro.au

Marina Pervukhina*

CSIRO
26 Dick Perry Ave
Kensington
WA 6151
Australia
marina.pervukhina@csiro.au

Jean-Baptiste Peyaud

CSIRO
26 Dick Perry Ave
Kensington
WA 6151
Australia
Jean-Baptiste.Peyaud@csiro.au

Yevhen Kovalyshen

CSIRO
26 Dick Perry Ave
Kensington
WA 6151
Australia
Yevhen.Kovalyshen@csiro.au

Valeriya Shulakova

CSIRO
26 Dick Perry Ave
Kensington
WA 6151
Australia
valeriya.shulakova@csiro.au

Mark Raven

CSIRO
Gate 4, Waite Rd
Urrbrae
Sth Aust 5064
Australia
mark.raven@csiro.au

Lionel Esteban

CSIRO
26 Dick Perry Ave
Kensington
6151 WA
Australia
Lionel.Esteban@csiro.au

SUMMARY

Overburden shales that overlie and seal hydrocarbon reservoirs usually exhibit polar anisotropy, also called Vertical Transverse Isotropy (VTI). This anisotropy is important for correct seismic inversion, seismic-to-well ties as well as having geomechanical implications. P-wave anisotropy cannot usually be determined from a vertical well unless a walkaway vertical seismic profile (VSP) has been obtained, however, such measurements are still rare. S-wave anisotropy though can be estimated from logs if the speed of sound in mud and the Stoneley wave velocity in the shale are known. Then, the P-wave anisotropy can be computed using theoretical models or empirical trends. The Stoneley wave velocity is nowadays routinely measured by sonic tools and, if a reliable mud velocity is known, the horizontal shear wave velocity (parallel to and polarised in the bedding plane) can be estimated. Thomsen's gamma parameter for S-wave anisotropy can then be calculated. If mud velocity is not known, the horizontal shear wave velocity can be obtained using calibration in an isotropic interval. Using this method, we analyse the VTI anisotropy in the Torosa-6 well in the Caswell Sub-basin of the Browse Basin, Australia. Torosa-6 drilled through the Jamieson and Echuca Shoals shaly formations where V_{clay} reaches ~75%. Elastic anisotropy of the shaly Jamieson and Echuca Shoals Formations has been analysed. Thomsen's gamma shows a good correlation with the clay fraction in each of these formations. However for the same clay fraction, anisotropy is about 20% higher in the Jamieson Formation compared to the Echuca Shoals. This Jamieson Formation contains up to 15% of smectite, and we are investigating how this may lead to higher levels of VTI anisotropy compared with illitic clays predominant in the Echuca Shoals Formation.

Key words: VTI anisotropy, Jamieson Formation, Browse Basin

INTRODUCTION

Hexagonal anisotropy with a vertical symmetry axis (so called, polar or Vertical Transverse Isotropy, VTI anisotropy) is ubiquitous in the upper crust. In the past, anisotropy was commonly neglected due to complexity of the mathematical apparatus and associated ill-posed inversion problems and is still often neglected due to lack of reliable information. Nevertheless it is known that ignoring VTI anisotropy causes substantial errors in both imaging and reservoir characterization, and taking it into account is essential to reduce exploration uncertainty. As an improved understanding of VTI anisotropy results in reduced exploration risk and better characterization of conventional and unconventional oil and gas reservoirs, here we analyse its origin on an example of the anisotropic Jamieson and Echuca Shoals Formations, the Browse Basin.

The VTI anisotropy might stem from the presence of organic-rich source rocks, omnipresent shales and cracks/fractures/fracture corridors to name just a few. The anisotropy can be scale dependent and as a consequence differ from the anisotropy measured at core scale. At the same time, characterization of seismic anisotropy at a larger scale is challenging as this requires walk-away vertical seismic profiles or far-offset seismic data which are not regularly acquired (and whose analysis is challenging and prone to errors). As the studies of VTI anisotropy at a large scale are rare, some authors attempt to attribute it to mechanical and chemical compaction only (e.g., Bachrach, 2011; Dræge et al., 2006; Johansen et al., 2004). However, other studies show that mineralogy and the depositional environment of the rocks has a first order effect on VTI anisotropy (Mondol et al., 2007; Pervukhina et al., 2015; Beloborodov et al., 2016), while the compaction has a second order effect on it (Pervukhina and Rasolofosaon, 2017).

Here we explore an opportunity to calculate the VTI anisotropy from Stoneley wave. First, five wells in the Torosa gas field in the Browse Basin are identified and the Stoneley waveforms processed to calculate the Stoneley wave velocity if it was not provided with

the service companies. Second, the mud velocity is obtained by calibration on an interval that assumed to be isotropic and the shear velocity that propagates and polarised within the bedding plane is calculated using the Stoneley wave velocity and the mud velocity. Then the shear wave anisotropy, γ , is calculated in the shaly Jamieson and Echuca Shoals Formations. To understand the main reasons that cause VTI anisotropy, the obtained γ is compared with the XRD mineralogy results that obtained on the cuttings from Torosa 6 well, where the thickness of the Jamieson and Echuca Shoals Formations is ~500 meters. The available geological information about the depositional environment in the Browse Basin is also taken into account.

GEOLOGICAL CONTEXT

Browse basin and Torosa field location

The Browse Basin is an extensional northeast-southwest trending basin covering 140000 km² area offshore of the Australia's North West Shelf. It includes the Caswell, Barcoo and Seringapatam sub-basins, the Scott Plateau, and the Yampi and Leveque shelves (Figure 1). The main depocentre is the Caswell Sub-basin which contains a Paleozoic, Mesozoic and Cenozoic sedimentary succession over 15 000 m thick (Geoscience Australia, 2017).

The Browse basin is considered to be a world-class gas province with proven reserves estimated at 910.77 Billion cubic meters of gas and 1.79 MMbbl of crude oil (Geoscience Australia, 2012). As a consequence, it is a major target for exploration and production in Australia. The main hydrocarbon accumulations are located in the Caswell sub-basin including the Torosa gas field (Figure 1), one of the major fields with Ichthys-Prelude-Concerto.

The North West margin dynamics

The first major extension event occurred in the late Carboniferous - Early Permian and resulted in the formation of the Neo-Tethys (Veevers et al., 1991). It initiated the formation of the Westralian Superbasin which includes the Browse basin (Yeates et al., 1987). This extension was oriented to the NW-SE and set up the predominant fault trend in the Browse basin. The basin was structured as a serie of intracratonic extensional half graben delimited by large-scale normal faults with two major depocentres in the Caswell Sub-basin and Barcoo Sub-basin (Figure 1) (Rollet et al., 2016).

The late Paleozoic rifting phase was followed by a period of thermal subsidence during the Permian and Triassic (Struckmeyer et al., 1998) that resulted in the deposition of thick packages of shallow marine to deltaic and fluvial sediments over the whole of the Browse basin. A first compressional event during the late-Triassic caused a partial inversion of the half-grabens in the Barcoo and Caswell sub-Basin. This generated large-scale northeast-trending anticlinal and synclinal structures in the Caswell Sub-Basin and a more subtle deformation in the Barcoo sub-Basin (Kennard et al., 2004, Rollet et al., 2016).

In the Early-middle Jurassic, the North West margin was affected by a major phase of rifting oriented ENE-WSW that resulted in the separation of the Indian and Australian plates. Heine and Muller (2006) and Hall (2012) showed that the spreading started in the Argo abyssal plain and then propagated to the Bonaparte and the Browse basin during the Oxfordian. This extension was critical for the structuration of the Browse Basin and by the end of the Jurassic (Lawrence, 2014) its main structural trends were established. The Early-Middle Jurassic syn-rift sediments are represented by the Plover formation that consists of sandstones, mudstones and coals deposited in a deltaic to coastal-plain environment (Kennard et al., 2004). The Plover Formation presents both source rocks and reservoir formations.

The Late Jurassic to Early Cretaceous was a period of transition of the Browse basin from an intracratonic rift basin to a passive margin. A prolonged phase of thermal subsidence affected the whole area until the Early Miocene, leading to the deposition of large sedimentary packages (Lawrence, 2014; Rollet et al., 2016). The geological succession studied in this work was deposited at the beginning of this period and consist of two thick formations of marine claystones, the Echuca Shoals and Jamieson formations. Lissn and Sheng He (2012) describe the overlying post rift sequences in details.

A final minor inversion affects the North West Margin during the Middle-Late Miocene. Longley et al., (2002) suggest it occurred as a consequence of the convergence between Australia and South-East Asia.

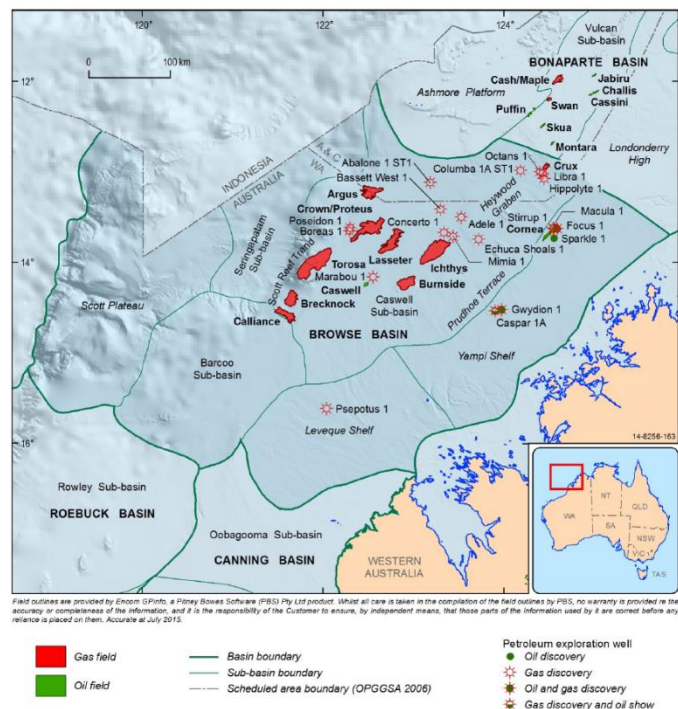


Figure 1. Geographic location and hydrocarbon accumulations of the Browse Basin (Rollet et al., 2016)

Studied wells and formations

The Torosa field (Figure 2) holds a significant fraction of the total basin gas reserves currently estimated at 37 % (Lawrence, 2014). Nine wells were drilled in this field during two periods. The Scott Reef wells were spudded between 1971 and 1982 and were followed by the Torosa wells drilled between 2006 and 2008.

The formations of interest to this study are two thick shale units called the Jamieson and Echuca Shoals formations. The latter was encountered only in Torosa 3, Torosa 5 and Torosa 6. The Jamieson formation has been intersected in all the wells but with significant variations in thickness. Only the base of the formation was present in Torosa 3 while only 50 m occurred in Torosa 1. The Vulcan formation would have constituted a potential target for this study but it was discarded as its thickness is low and it does not occur in all the wells (Figure 3).

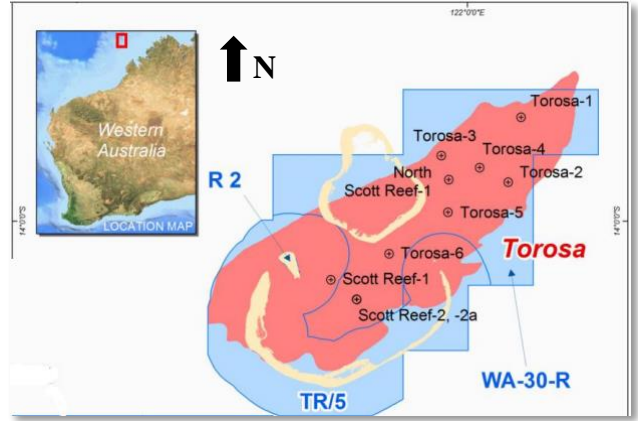


Figure 2. Well locations in the Torosa gas field (Woodside report, 2014)

Data available

Most of the data used for this work is publicly available from the National Offshore Petroleum Information Management System (NOPIMS) and the Western Australia Petroleum & Geothermal Information Management System (WAPIMS). It consists mostly of conventional well log data including Gamma Ray (GR), resistivities, density, porosity and acoustic measurements (compressional, shear and Stoneley wave velocity/slowness). The formation tops were obtained from the well completion reports for the Torosa wells. These reports also provided information on the sedimentology of the formations and their depositional environment.

In addition to this data, 14 cutting samples collected with a spacing of 10 to 25 m from Torosa 6 were analysed by XRD to characterize their bulk mineralogical composition. Samples were chosen based on the observed variations of the Thomsen γ estimation, which are described in the following section. They were analysed at the CSIRO Land and Water laboratories in Adelaide. Samples were hand-picked to ensure visually homogeneity, then they were crushed and analysed as dispersed powders according to the laboratory standard protocol. 1.5 g sub-samples were ground for 10 minutes in a McCrone micronizing mill under ethanol. The resulting slurries were oven dried at 60°C then thoroughly mixed in an agate mortar and pestle before being lightly pressed into aluminium sample holders for X-ray diffraction analysis. XRD patterns from the micronized materials showed variable hydration of the interlayer which causes problems with quantification. As the samples did not appear to contain any water soluble phases they were calcium saturated and the data re-analysed.

METHODOLOGY

Analytical protocol

A standard set of processed sonic tool measurements consist of (i) velocity of compressional wave (P-wave) propagating along the borehole and (ii) velocity of shear wave (S-wave) propagating along the borehole. Sometimes service companies also provide velocity of the Stoneley wave, a low frequency tube wave propagating through the annulus space between the tool and the borehole walls. Note that for Stoneley wave measurements service companies use a specific low-frequency source. The Stoneley wave velocity depends on the mud velocity and the velocity of shear wave propagating and polarized in the plane normal to the well. If the sound velocity in the mud is known, this shear wave velocity of surrounding wave can be obtained. In the presence of tool, the Stoneley velocity is given by (White, 1983) as follows:

$$V_{S\perp} = \left[\left(1 - \frac{R_{tool}^2}{R_{well}^2} \right) \frac{\rho_{rock}}{\rho_{mud}} (V_{st}^{-2} - V_{mud}^{-2}) \right]^{-1/2}$$

where V_{mud} is the velocity of compressional waves in the mud, $V_{S\perp}$ is the velocity of shear wave propagating and polarized in the plane that is perpendicular the well, ρ_{mud} and ρ_{rock} are the mud and rock densities respectively, R_{tool} and R_{well} are the radii of the tool and well respectively. Note that in the case of vertical borehole drilled normal to the bedding, the $V_{S\perp}$ is the velocity propagating and polarized in the bedding plane.

Knowing Stoneley wave velocity V_{ST} one can get $V_{S\perp}$. Then using velocity shear wave propagating along the borehole, one can estimate rock anisotropy through Thomsen's γ (Thomsen, 1986):

$$\gamma = 0.5 \left(\frac{V_{S\perp}^2}{V_{S\parallel}^2} - 1 \right)$$

In the presented here analysis V_{ST} and $V_{S||}$ were taken from sonic logs, ρ_{rock} from density log, ρ_{mud} and R_{tool} from well completion reports, R_{well} from the calliper log, and V_{mud} was calculated from a isotropic section. The variation of the Thomsen's γ was then compared to the conventional logs in each wells and between the different wells. It was also compared to the mineralogical composition obtained from XRD analysis of cutting samples.

RESULTS

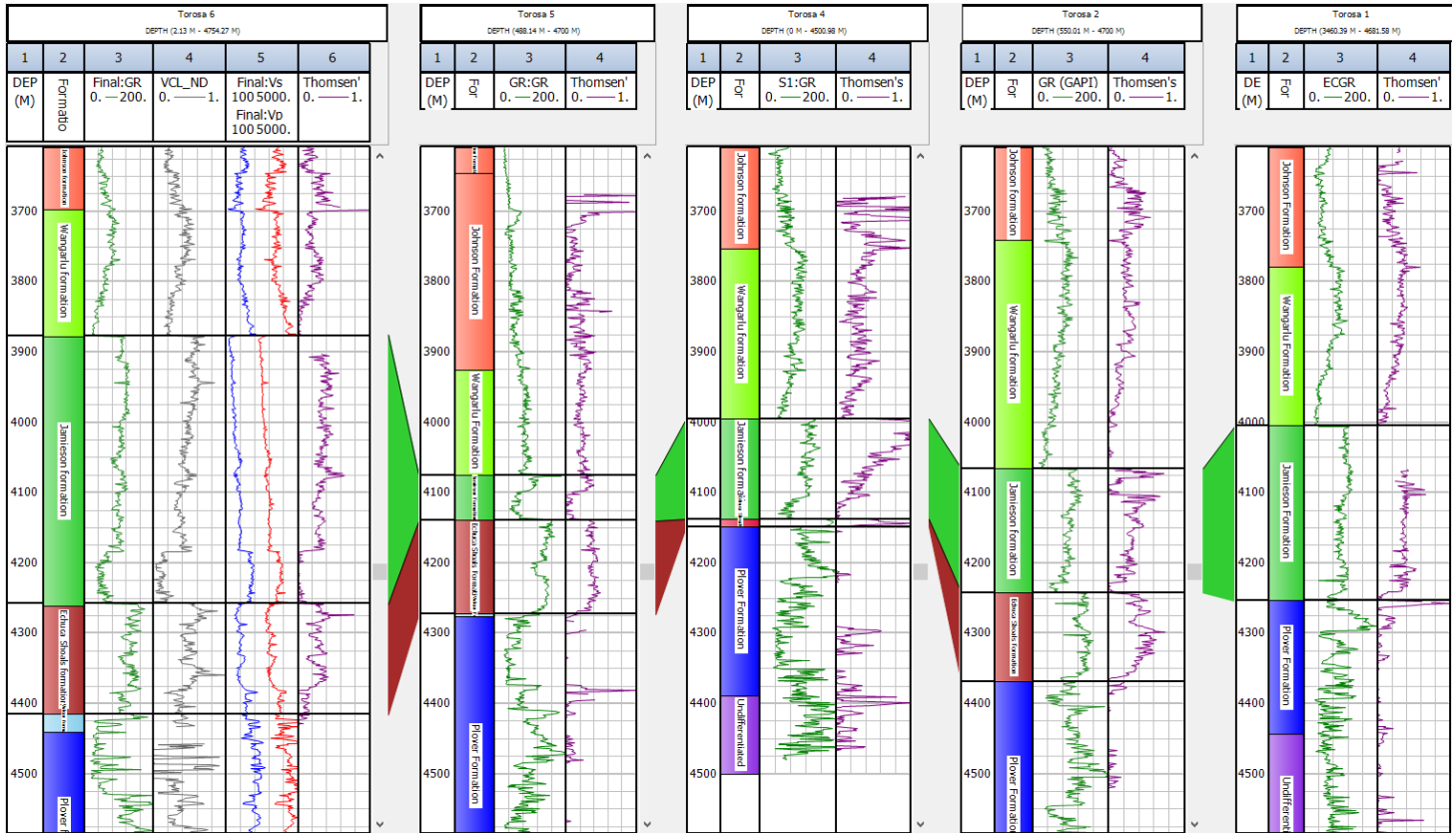


Figure 3. GammaRay (green) and Thomsen γ (purple) well data correlation in Torosa 6-5-4-2-1 wells, the correlation has a SW-NE direction

Figure 3 shows vertical profiles of calculated S-wave anisotropy (γ) in five wells in Torosa field, namely, Torosa 1, Torosa 2, Torosa 4, Torosa 5 and Torosa 6. We pay a particular attention to Torosa 6 as in this well the thickness of the shaly Jamieson and Echuca Shoals Formations are maximum. The Torosa-6 curves display the GR, the calculated volume of clay (VCL), acoustic measurements and γ variations respectively from the tabs 3 to 6 (figure 3). The volume of clay was calculated based on the neutron and density porosity separation and calibrated with the XRD analysis results. The S-wave anisotropy (γ) broadly follows the same variation with the GR and VCL. As is the either Jamieson or Echuca Shoals Formations, the volume of clay decreases with the depth increase, the S-wave anisotropy shows negative trends in both formations. In Torosa 6, the γ does not exceeds 0.8 with this maximum value reached at the Echuca Shoals and with the median value of ~ 0.4 . The lower maximum value of 0.6 is reached in Jamieson Formation. The minimal value of 0 is reached at the bottom of Jamieson Formation, in the interval that is assumed to be isotropic and is used for calibration.

In spite of a relatively small distances between the wells, the lateral variations in the γ values are quite significant. Generally, these variations are related to the lateral variations in the Jamieson and Echuca Shoals Formation thicknesses caused presumably by erosion. While the shear wave anisotropy tends to increase when the GR increases, no specific trend with the depth increase is observed. For instance in the Torosa 6 well, both GR and γ decrease with the depth increase.

As Torosa 6 well penetrates through approximately 500 metres of the shaly Jamieson and Echuca Shoals Formations where the S-wave anisotropy shows some prominent variations, the cuttings from this well were selected to understand mineralogical differences that could affect it. XRD analysis has been done on 14 samples selectively collected from the Jamieson and Echuca Shoals Formations to

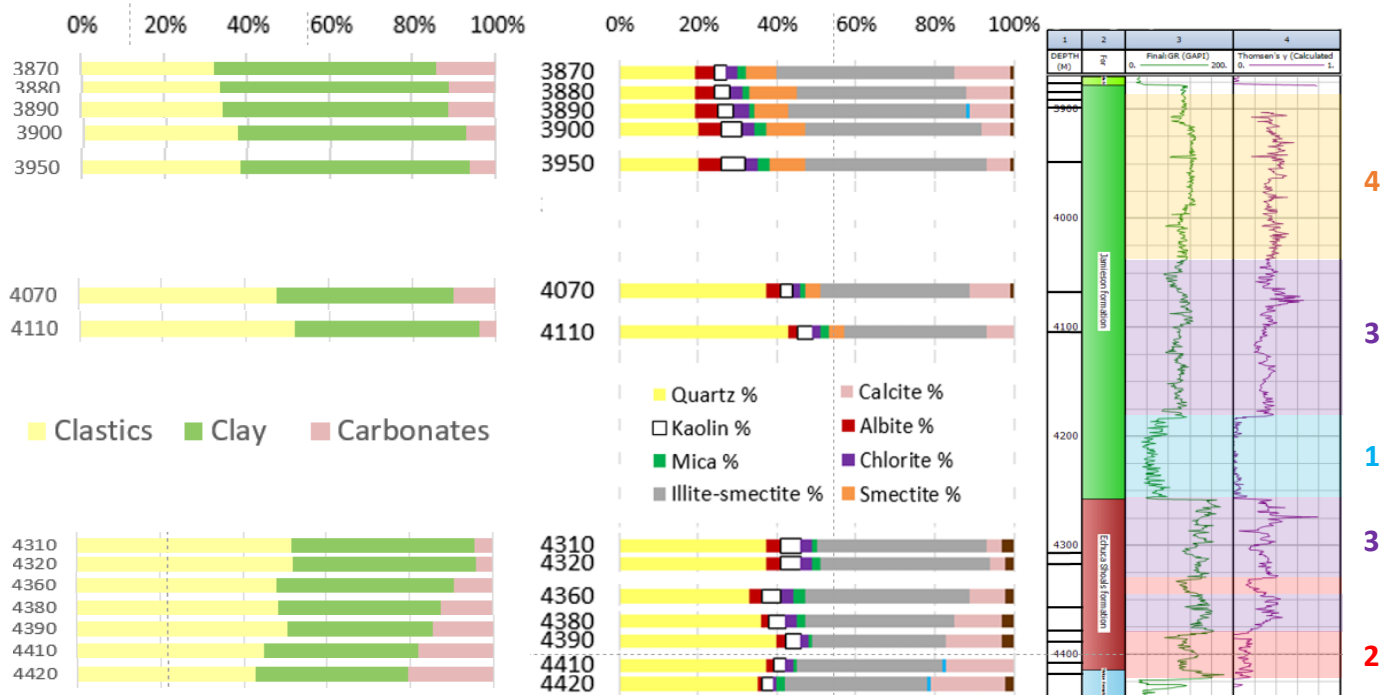


Figure 4. Quantitative mineralogy of the cutting samples from Jamieson and Echuca Shoals formations in Torosa-6 well, the minerals proportions are added together according to their type (clastic, clay or carbonate) in the left diagram. The profile on the right shows the intervals based on the relative variation between γ and shear velocity.

understand their mineralogical composition (Figure 4). The top of the Jamieson formation appears to be more argillaceous with above 32% clastics, 55% clay minerals and 13% carbonates. The base of the Jamieson has more clastics (about 50%), less clay minerals (about 40%) and less than 10% calcite. By comparison, the Echuca Shoals Formation is more homogeneous with about 45% quartz and feldspars, clay minerals decreasing from about 50% to about 40% from the top of the formation toward its base and carbonates increasing from 5 to 20%. Dolomite was observed at the base of the Echuca Shoals and at 3890 m in the Jamieson Formation: its occurrence is discrete. Besides the bulk amount of clay minerals, another difference between the Jamieson Formation and the Echuca Shoals is the occurrence of up to ~15% of smectite as a discrete phase in the Jamieson Formation while it only occurs as mixed layers in the Echuca Shoals. The amount of kaolinite seems relatively constant between 5 and 10% throughout the series, the amount of chlorite does not exceed 5%. Mixed-layers illite-smectite constitute the major clay mineral in the study interval.

Discussion

To understand how clay fraction, clay mineralogy and other factors affect VTI anisotropy, the variation of the Thomsen γ is plotted as a function of 4 log parameters: the GR, the shear velocity, the volume of clay and the V_P/V_S ratio (Figure 5). Compared to the GR (Figure 5.A), the Thomsen γ is distributed in three groups. One group characterized by γ values below 0.2 and GR below 80 corresponds to the sandstones at the base of the Jamieson Formation (4175–4250 m). The points with γ below 0.2 and a GR below 120 in the Echuca Shoals Formation are expected to correspond to the silty intervals at 4330–4350 m and 4380–4420 m. The other two groups show a tendency of the GT to increase with increasing GR in both the Echuca Shoals and the Jamieson Formations. However, for a similar range of γ , the level of GR is higher in the Echuca Shoals, suggesting that the relation between GR and γ is not simple and direct.

The comparison between the Thomsen γ and the S wave velocity (Figure 5.B) shows a strong negative trend and an isolated group of points with γ varying between 0.5 and 0.3 and velocities between 1300 and 1500 m/s. The negative trend indicates that γ decreases with increasing acoustic velocity. The isolated group of points corresponds to the top 150 m of the Jamieson formation where the highest abundance of smectite clay minerals was observed.

The comparison between the volume of clay (VCL) and the Thomsen γ show two isolated groups from the rest of the points (Figure 5.C). The first group characterized by γ values below 0.2 and VCL below 20% corresponds to the siltstones at the base of the Jamieson formation (4182–4257 m) (**Error! Reference source not found.** 5). The points with a γ below 0.2 and a VCL between 30 and 50 % form the second group. They correspond to the intervals at 4330–4345 m and 4375–4415 m (Figure 5).

The principal group of points have a γ above 0.2. They show a tendency of the γ to increase with increasing VCL in both the Echuca Shoals Formation and the Jamieson. Considering all points with a γ above 0.2, the Jamieson formation appears to be more anisotropic. The VCL is similar between the formations which display a common variation range between 40% and 60%.

The crossplot between the Vp/Vs ratio and γ shows that anisotropy increases almost linearly with the Vp/Vs ratio increase (Figure 5.D). The points could be grouped into at least three different clusters. The first cluster, characterized by γ below 0.2, corresponds to the sandstones at the base of the Jamieson formation and the siltstones in the Echuca Shoals and shows the typical for these rocks values of Vp/Vs ratio of 1.6-1.8. The cluster of the points with γ above 0.2 can be further subdivided in a group with Vp/Vs below 2.3 that contains points from both formations and a group with Vp/Vs above 2.3 containing points mostly from the Jamieson formation.

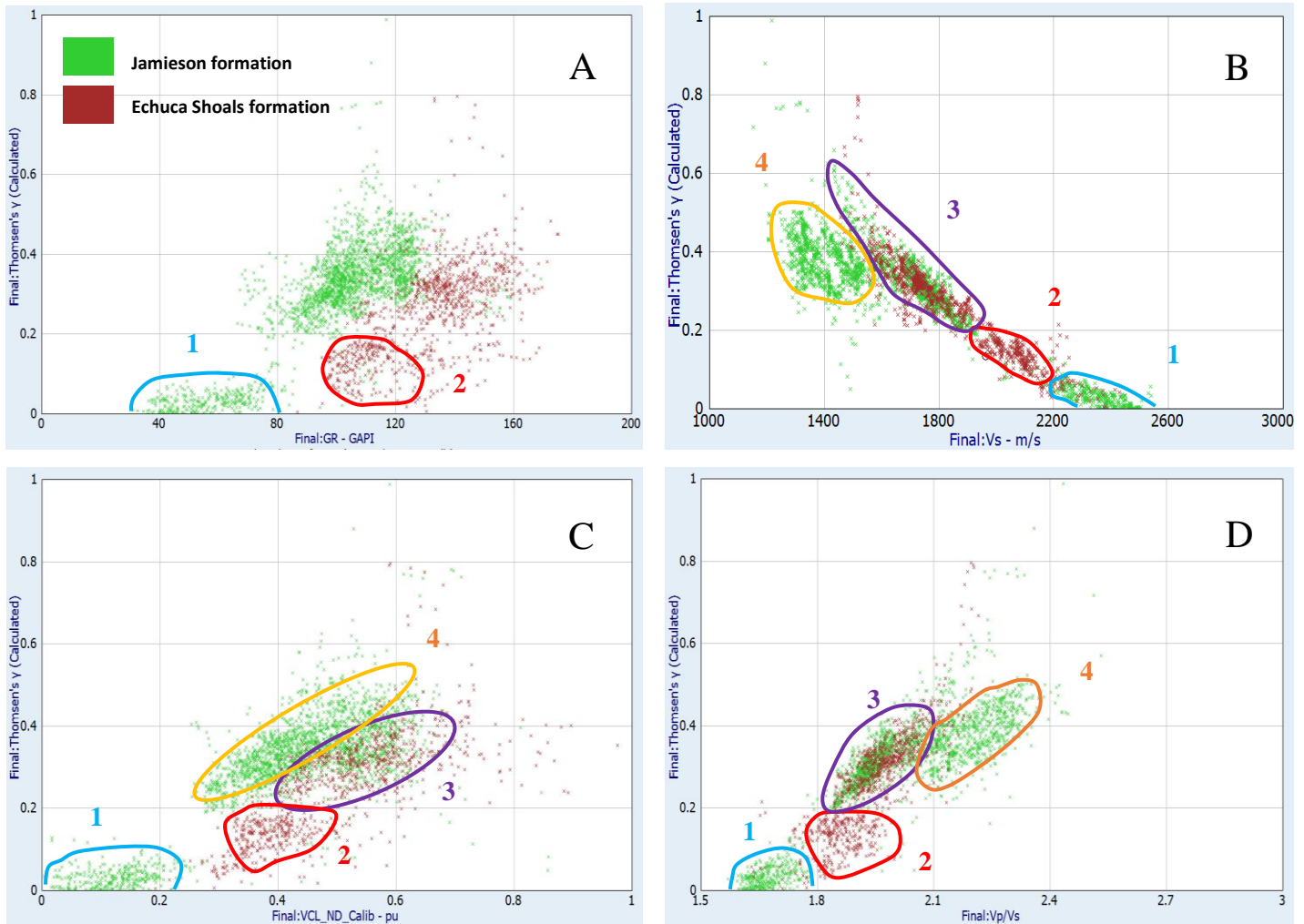


Figure 5. Thomsen γ variation depending on the GR (A), Vs (B), calculated clay volume (C) and Vp/Vs (D). The data from Jamieson and Echuca Shoals Formation are shown by green and brown markers, respectively.

As already mentioned, no correlation is observed between the depth and anisotropy. In Torosa 6 well, the average value of the Thomsen γ in the Echuca Shoals is lower than the one in Jamieson Formation that overlies it. If a correlation between γ and depth of burial exists it has a second order effect compared to variations in rock mineralogy.

The γ tends to follow the variation of the GR which implies that the clay content has a major effect on elastic anisotropy. According to the XRD results, the top of the Jamieson Formation displays the highest clay content and the highest level of anisotropy. The lower parts of the Jamieson and the Echuca Shoals Formations, where the amount of quartz and carbonate is higher, display lower values of anisotropy. This shows that the clay content is positively related to the elastic anisotropy as was reported in studies conducted on artificial shale samples with controlled clay content (e.g., Beloborodov et al., 2016; Mondol et al., 2007). The type of clay minerals could also have an effect: the Jamieson Formation contains smectite as a discrete occurrence while it is only present in mixed layers in the Echuca Shoals. The different groups of points (1, 2, 3, 4) indicated in Figure 5 correspond to the depth intervals indicated in Figure 4. These intervals are consistent with the variation of mineralogical composition.

Both the Jamieson and the Echuca Shoals formations were deposited in a marine environment. Based on micropaleontological data, the Jamieson Formation was deposited in a deeper, mid-bathyal environment while the Echuca Shoals was deposited in a shallower, offshore environment. This is consistent with the higher clay content observed in the Jamieson Formation and the higher quartz content

in the Echuca Shoals. Based on the logs (Figure 3) and the crossplots in Figure 5, the γ tends to increase in more argillaceous formations and would thus be more intense in layers deposited in deeper and quieter environments.

Besides the mineralogical composition, there are a number of other factors that could affect the anisotropy values, for instance, the extent of compaction, the thin lamination below the sonic log resolution, the dip of the bedding or the grain size distribution. Elements related to the texture of the formation or its physical heterogeneity like bed thickness and layering frequency were not tested in this study due to a lack of data (no cores nor image logs available).

CONCLUSIONS

The S-wave anisotropy of the Jamieson and Echuca Shoals Formations that contain significant amount of shale have been analysed in five wells drilled in the Torosa field in the Browse Basin. The obtained elastic anisotropy shows strong positive trend with the clay content. The obtained dependencies of S-wave anisotropy γ on clay content are different in the Jamieson and Echuca Shoals Formations with the values of elastic anisotropy higher in the Jamieson Formation compared to the Echuca Shoals for the same values of clay content. This difference is explained with the observed difference in clay mineralogy i.e., presence of smectite in Jamieson Formation. This difference can be also related to the difference in depositional environment, namely, deep or shallow marine in the case of Jamieson and Echuca Shoals, respectively. Burial depth has been shown to have a second order effect on elastic anisotropy either within a single formation, where the anisotropy is mostly affected with clay content, or between different formations. The variation of γ with Vs is non-monotonous with the maximum values at ~1500 m/s. The anisotropy decrease at larger velocities is explained with the increase of quartz and calcite fractions; the decrease of anisotropy at lower velocities is implied to be related to possible overpressure.

REFERENCES

- Geoscience Australia, Offshore Petroleum Exploration Acreage Release, 2012, 2017.
- Beloborodov, R., Pervukhina, M., Luzin, V., Delle Piane, C., Clennell, M.B., Zandi, S. and Lebedev, M., 2016. Compaction of quartz-kaolinite mixtures: The influence of the pore fluid composition on the development of their microstructure and elastic anisotropy. *Marine and Petroleum Geology*, 78, pp.426-438. (1).
- Heine, C., and Müller, R.D., 2005, Late Jurassic rifting along the Australian North West Shelf: margin geometry and spreading ridge configuration, *Australian Journal of Earth Sciences*, 52:1, 27-39
- Hall, R., 2012, Late Jurassic-Cenozoic reconstructions of the Indonesian region and the Indian Ocean. *Tectonophysics*, 570 (1), 1–41
- Kennard, J.M., Deighton, I., Ryan, D., Edwards, D.S. & Boreham, C.J., 2004. Subsidence and thermal history modelling: new insights into hydrocarbon expulsion from multiple systems in the Browse Basin. In: Ellis, G.K., Baillie, P.W. and Munson, T.J. (eds.): *Timor Sea Petroleum Geoscience. Proceedings of the Timor Sea Symposium*, Darwin. Northern Territory Geological Survey. Special Publication 1, 411-435.
- Lawrence, S.H.F., Thompson, M., Rankin, A.P.C., Alexander, J.C., Bishop, D.J., and Boterhoven, B., 2014, A new structural analysis of the Browse Basin, *Australian North West Margin*.
- Lisssn, N.H. & He, S., 2012. Source rocks thermal evaluation and burial history reconstruction in the Caswell Sub-basin, Northwest Shelf, Australia. *Nature and Science*, 10(2), 124-141.
- Longley, I.M., Buessenschuett, C., Clydsdale, L., Cubitt, C.J., Davis, R.C., Johnson, M.K., Marshall, N.M., Murray, A.P., Somerville, R., Spry, T.B. & Thompson, N.B., 2002. The North West Shelf of Australia; a Woodside perspective. In: Keep, M. & Moss, S.J. *The Sedimentary Basins of Western Australia 3: Proceedings of Petroleum Exploration Society of Australia Symposium*. Petroleum Exploration Society of Australia, Perth. 27-88.
- Mondol, N.H., Bjorlykke, K., Jahren, J., Hoeg, K., 2007. Experimental mechanical compaction of clay mineral aggregates - changes in physical properties of mudstones during burial., *Mar. Pet. Geol.* 24, 289-311.
- Pervukhina, M. and Rasolofosaon, P. N.J. (2017), Compaction trend versus seismic anisotropy in shaly formations. *Geophysical Prospecting*. doi:10.1111/1365-2478.12486 (1).
- Rollet, N., Abbott, S.T., Lech, M.E., Romeyn, R., Grosjean, E., Edwards, D.S., Totterdell, J.M., Nicholson, C.J., Khider, K., Nguyen, D., Bernardel, G., Tenthorey, E., Orlov, C., and Wang, L., 2016, A regional assessment of CO2 storage potential in the Browse Basin, Results of a study undertaken as part of the National CO2 Infrastructure Plan, RECORD 2016/17
- Stagg H. M. J., Wilcox J. B., Symonds P. A., O'Brien G. W., Colwell J. B., Hill P. J. A., Lee C-S., Moore A. M. G. and Struckmeyer H. I. M. 1999. Architecture and evolution of the Australian continental margin. *AGSO Journal of Australian geology & geophysics* 17, 17 – 33.
- Struckmeyer, H.I.M., Blevin, J.E., Sayers, J., Totterdell, J.M., Baxter, K. & Cathro, D.L., 1998. Structural evolution of the Browse Basin, North West Shelf: New concepts from deep-seismic data. In: Purcell, P.G. & Purcell, R.R. (eds.) *The Sedimentary Basins of*

Western Australia 2: Proceedings of the Petroleum Exploration Society of Australia Symposium. Petroleum Exploration Society of Australia, Perth. 345-366.

Torosa-1 well completion report, 2007, V. Sturrock, Woodside

Torosa-2 well completion report, 2007, V. Sturrock, Woodside

Torosa-3 well completion report, 2007, V. Sturrock, G. Hamson, Woodside

Torosa-4 well completion report, 2008, Jodie Monro, Woodside

Torosa-5 well completion report, 2009, V. Sturrock, Operations Geology. Woodside

Torosa-6 well completion report, 2009, V. Sturrock, Operations Geology. Woodside

Thomsen L. 1986. Weak elastic anisotropy. *Geophysics* 51(10), 1954–1966.

Veevers, J.J., Powell, C.McA., and Roots, S.R., 1991, Review of seafloor spreading around Australia. I. synthesis of the patterns of spreading, *Australian Journal of Earth Sciences*, 38:4, 373-389

White, J.E., 1983. *Underground Sound - Application of Seismic Waves*. Amsterdam: Elsevier.

Woodside Energy, 2014, First Order Analytical Estimates of Scott Reef Subsidence as a result of Reservoir Compaction in the Torosa Field, Browse Basin, Appendix F39

Yeates, A.N., Bradshaw, M.T., Dickins, J.M., Brakel, A.T., Exon, N.F., Lanford, R.P., Mulholland, S.M., Totterdell, J.M. And Yeung, M., 1987, The Westralian Superbasin, an Australian link with Tethys. In: Mckenzie, K.G. (ed.) *Shallow Tethys 2: International Symposium on Shallow Tethys 2*, Wagga Wagga, NSW, (1987), 199–213.